

# The $t$ system: a new system for estimating the total magnitudes of galaxies

Christopher Ke-shih Young<sup>1</sup>, Nigel Metcalfe<sup>2</sup>, Jin Zhu<sup>1</sup>, Hong Wu<sup>1</sup> and Jian-sheng Chen<sup>1</sup>

<sup>1</sup>Beijing Astronomical Observatory, Chinese Academy of Sciences, Beijing 100080, China

<sup>2</sup>Department of Physics, University of Durham, South Road, Durham DH1 3LE, England

Accepted 1997 November 12

**Abstract.** We present a new, but simple, procedure for estimating the total magnitudes of galaxies. This procedure involves the out-focusing of digital galaxy images numerically, the fitting of the resulting surface-brightness profiles with a *single* generalised profile model and the extrapolation of the fitted profiles to infinite radial distances. This new system, which we denote  $t$ , differs fundamentally from the  $T$  system (of the *Reference Catalog of Bright Galaxies* series) in that: (1) it enables a galaxy's luminosity profile to be extrapolated without the need for any prior morphological classification, and (2) it is applicable to images of widely different spatial resolutions (including unresolved ones) because it takes into account systematic effects due to differential image resolution. It also differs fundamentally from the Kron system in that: (1) it can be derived directly from surface photometry without the need to go back to the plate scans or CCD frames (unless the surface photometry is of high resolution and/or the galaxies being measured are very bright), and (2) it can cope with merged images (provided they are separable by image-segmentation software). Through worked examples, we demonstrate the stability of  $t$ -system total magnitudes with respect to morphological type, the seeing conditions at the time of observation, degree of smoothing and limiting isophote. We also compare and contrast the new system with both the  $T$  system and the Kron system, and investigate the advantages and limitations of each of the three systems.

**Key words:** Atmospheric effects – Methods: data analysis – Methods: observational – Galaxies: fundamental parameters – Galaxies: photometry

## 1. Introduction

At sufficiently large angular distances from the centre of any galaxy image, the surface-brightness contribution due to the galaxy becomes, at some point, indistinguishable from the surface-brightness of the surrounding sky. The limit on reliable observation is determined primarily by the noise and often corresponds to those points at which the galaxy's surface brightness has fallen to several percent of the sky, though limits in the region of 0.1% of the sky are measurable on occasions.

Although total magnitudes are required for many astrophysical applications, it is therefore not possible to measure them directly. Instead, estimates are normally obtained by means of extrapolating model profiles fitted to those parts of the galaxy-light profiles (whether surface-brightness or integrated) that can be measured reliably. However, galaxies of different morphological type have very different profile shapes, and a wide range of models have generally had to be invoked. In Kron's (1980) system though, the flux due to a galaxy is measured to *very* large radial distances, so that different models do not need to be invoked. Such a procedure has its advantages, but at the very large radial distances involved, the signal due to the galaxy is often such a small fraction of the noise that large random errors cannot be avoided.

An alternative approach to profile extrapolation is *very*-low-resolution imaging so that, in theory at least, all target galaxies essentially become point sources and yield images of almost identical structure. Total magnitudes then become a simple function of the full-width half maximum (FWHM) of the image point-spread function. In practice, the FWHM of the point-spread function has to be much larger than the intrinsic angular sizes of the target galaxies for this method to yield reliable magnitudes. However, the wider the point-spread function is, the lower the mean surface-brightness of each image becomes and the greater the errors due to the noise become. In the compilation of their *Catalog of Galaxies and Clusters of Galaxies*, Zwicky et al. (1961, 1963, 1965, 1966,

---

Send offprint requests to: C.K. Young by e-mailing c.young1@physics.oxford.ac.uk

1968) measured their total magnitudes visually from *out-of-focus* photographic plates. Out-of-focus images generally have a complicated point-spread function, but as long as they exhibit little variation across a single plate or CCD frame, this should not be a problem.

The new system presented in this paper combines both approaches. We believe that it can yield very large numbers of reliable total-magnitude measurements very efficiently, and that it is therefore particularly suitable for galaxy-survey work.

## 2. Existing extrapolation methods

In his pioneering study, Hubble (1930) found that the surface-brightness profiles of elliptical galaxies (which he measured along either the major or minor axes) seemed to be well fitted by the law:

$$\sigma(r) = \frac{\sigma_H}{(1 + \frac{r}{r_H})^2}, \quad (1)$$

where an elliptical-galaxy profile can be uniquely described by two terms:  $\sigma_H$  (a central surface brightness) and  $r_H$  (a scale length). The main problem with this law is that its integrand with respect to  $r$  diverges as  $r$  increases, and it is therefore unsuitable for extrapolation to large  $r$ .

An alternative representation was proposed by de Vaucouleurs (1948):

$$\sigma(r) = \sigma_e \operatorname{dex} \left\{ -3.33 \left[ \left( \frac{r}{r_e} \right)^{\frac{1}{4}} - 1 \right] \right\}, \quad (2)$$

where an elliptical-galaxy profile can be uniquely specified by  $r_e$  (the effective radius which contains half the galaxy's light).  $\sigma_e$  is the surface brightness at  $r = r_e$ . This representation has the advantage of a convergent integrand:

$$2\pi \int_0^\infty \sigma(r)r \, dr = 22.4\sigma_e r_e^2, \quad (3)$$

However, it has the disadvantage that strictly, the total luminosity needs to be known before the effective parameters can be evaluated.

A move away from wholly empirical functions was made by King (1966). King's models were constructed with tidally truncated globular star clusters in mind but have also been applied to elliptical galaxies. They assume that at all points within a stellar system, the frequency distribution of stars as a function of position and velocity can be described by an isothermal Gaussian minus an offset. At any position within the system, the offset is chosen so as to ensure that the frequency distribution is zero for stars with velocities equal to and in excess of the local escape velocity. This succeeds in reducing an otherwise infinite isothermal space distribution of stars to one with a finite radius. Nevertheless, the empirical law of de Vaucouleurs actually offers a better description of tidally unperturbed galaxies than does King's model.

Despite the intricate structure exhibited by many spiral galaxies, it has long been realised, e.g. by de Vaucouleurs (1958) that their smoothed light profiles could be separated into two components: a central component approximately obeying an  $r^{\frac{1}{4}}$  law<sup>1</sup> (corresponding to the spheroidal bulge, denoted *s*) and a more extended component approximately obeying an exponential law (corresponding to the disc, denoted *d*):

$$\sigma(r) = \sigma_{e,s} \operatorname{dex} \left\{ -3.33 \left[ \left( \frac{r}{r_{e,s}} \right)^{\frac{1}{4}} - 1 \right] \right\} + \sigma_{0,d} \exp \left[ - \left( \frac{r}{r_{0,d}} \right) \right], \quad (4)$$

where  $\sigma_{0,d}$  (the central surface-brightness due to the disc alone) and  $r_{0,d}$  (the scale length of the disc component) uniquely describe the disc component. The contribution due to this exponential component decreases as one progresses from late-type spirals to earlier types, but is not completely absent from lenticular objects or even classical ellipticals.

This trend in galaxy-profile characteristics from early through late types was exploited by de Vaucouleurs et al. (1976, 1991) during the compilation of their *Second* and *Third Reference Catalogs of Bright Galaxies* (hereunder RC2 and RC3 respectively). Their elaborate and widely-used scheme for extrapolating both aperture and surface-photometry measurements of galaxies, in order to estimate total magnitudes, is known as the *T* system. Although the *T* system has been used successfully to extrapolate the profiles of well resolved images of classical galaxies, its applicability to dwarf galaxies (as well as ellipticals intermediate between true dwarfs and true classicals) and to low-resolution images (of all galaxy types) is questionable. There appear to be at least three major limitations to the *T* system, the main consequences of which are summarised by Young (1997) and will be dealt with in more detail by Young et al. (in preparation).

(1) The scheme does not take into account the possibility that galaxies with profiles steeper than exponentials exist. As is evident from Young & Currie (1994, 1995) many dwarfs have profiles that *are* steeper than exponentials and some even have profiles as steep as Gaussians. These objects are therefore beyond the scope of the *T* system which necessarily over-estimates their luminosities.

(2) A morphological classification must be attempted first in order to be able to select the most appropriate extrapolation model for each galaxy concerned. This is normally done by eye. Many non-classical elliptical galaxies (including some with some characteristics of irregulars) e.g. IC 3475, 3349, 3457 and 3461, were classified as  $r^{\frac{1}{4}}$ -law objects by de Vaucouleurs et al. (1976, 1991) and their

<sup>1</sup> de Jong (1996) has recently shown that bulge surface-brightness profiles actually obey a range of laws in which the index to which  $r$  is raised varies considerably and is often much higher than 0.25.

profiles extrapolated accordingly. In fact IC 3475 has a very exponential profile as demonstrated by Vigroux et al. (1976), and the other three objects listed have profiles slightly steeper than an exponential as demonstrated by Young & Currie (in press). This means that whilst these objects could be accommodated by the *T* system if it were treated as objects with exponential profiles, their luminosities were in fact severely over-estimated by of the order of 100% in both the RC2 and the RC3 (Young, 1997; Young et al., in preparation) because of limitations in the morphological typing procedure. The need to estimate the profile shape by eye before an extrapolation can be performed is therefore a serious short-coming of the *T* system.

(3) No account is taken of atmospheric or instrumental effects that degrade the resolution of a galaxy image and thereby modify its *measurable* surface-brightness profile. Clearly a low-resolution image of a particular galaxy is likely to have a more Gaussian-like profile than is a high-resolution image of the same galaxy. This makes the *T* system difficult to apply consistently to images of different resolution and even to images of almost identical galaxies at widely differing distances.

A worthy alternative to the *T* system has long been the Kron (1980) system, in which the rate of growth of the signal with respect to the signal itself is considered as a function of radial distance from the centre of each galaxy image. The light is then measured within a circular region of a radius corresponding to the point at which the logarithmic derivative of the light growth curve becomes smaller than the *same* upper limit for all target galaxies. In practice there are strong constraints on the suitable values for this limit, and the range of suitable values generally require an aperture of radius equal to about twice the effective (half-light) radius. The fraction of the total light within this aperture (which in practice is typically of the order of 95%) is then assumed to be constant for all galaxies, and total magnitudes can be obtained by extrapolating the measured aperture magnitude values by the same amount (which in practice simply means adding typically about  $-0.05$  mag. to each aperture magnitude).

The Kron system has two major advantages over the *T* system, namely that the magnitude measurement process is independent of galaxy morphological type and that atmospheric effects that degrade image resolution and distort galaxy luminosity profile shapes are taken into account. However, it does have at least three major drawbacks.

(1) Large random errors are present due to having to measure luminosity growth curves and [even harder] their derivatives, out to very large radial distances where the signal due to the galaxy is a very small fraction of the noise. Note that the Kron system does not take the signal-to-noise ratio as a function of radial distance into account at all. This can be a particularly serious problem when dealing with low-surface-brightness galaxies such as

dwarfs.

(2) The need for very large apertures restricts which objects can be measured in crowded fields when undesirable galaxy or stellar images lie adjacent to the target objects. For this reason the Kron system has mainly been applied to field galaxies rather than cluster ones.

(3) Unlike the *T* system which is based on aperture and surface photometry measurements that can be extracted from the literature in their published form, one cannot compute Kron-system total magnitudes without access to the original digital-image data.

Despite the existence of the elaborate *T* and Kron systems, most large machine surveys of galaxies have, understandably, adopted simpler algorithms for extrapolating large numbers of isophotal magnitudes to totals. In the APM Southern-sky Survey of Maddox et al. (1990) the majority of galaxy images were assumed to be seeing dominated, and therefore to have approximately Gaussian profiles (on average at least). This was a particularly efficient method, as knowledge of an isophotal magnitude and the angular area of that isophote was sufficient to specify the parameters of a Gaussian profile uniquely; as described in detail in Maddox et al. (1990). However, such an approach is only applicable to unresolved galaxy images from sufficiently small and/or sufficiently distant objects.

In addition to the extrapolation systems discussed in this section, there are of course others. However, such systems have generally only been applied to limited galaxy samples of a particular morphological type.

### 3. The *t* system

This system was first adopted by Young (1994) and Young & Currie (in press) in the compilation of their *Virgo Photometry Catalogue* (hereunder VPC); as well as by Young & Currie (1995), Drinkwater et al. (1996) and Young (1997); who all quote *t*-system total magnitude values from the VPC. The *t* system is a system for extrapolating surface-brightness profiles of sufficiently low resolution, to  $r = \infty$  where  $r$  is reduced radial distance ( $\sqrt{r_{major}r_{minor}}$ ). This means that high-resolution images (those of non-nucleated dwarf and intermediate ellipticals excepted) must be smoothed sufficiently *prior* to any surface-brightness profile being parametrized, but has the important advantage that low-resolution images can be measured even if their profiles are significantly distorted by e.g. seeing effects or poor sampling. Although alternative smoothing functions can be used, we recommend a [radially-symmetric two-dimensional] Gaussian function.

In order to generate an extrapolated total *t*-system magnitude from a low-resolution surface-brightness profile, Sérsic's (1968) law is adopted:

$$\sigma(r) = \sigma_0 \exp \left[ -\left(\frac{r}{r_0}\right)^n \right], \quad (5)$$

in which  $\sigma(r)$  is the surface brightness in linear units of luminous flux density at  $r$ ,  $\sigma_0$  is the central surface brightness and  $r_0$  is the angular scalelength. The extrapolated central surface brightness is therefore:  $\mu_0 = -2.5 \log_{10} \sigma_0$  in mag.arcsec<sup>-2</sup>, whence the equivalent expression in logarithmic surface-brightness units is:

$$\mu(r) = \mu_0 + 1.086 \left( \frac{r}{r_0} \right)^n, \quad (6)$$

enabling values of  $\mu_0$  and  $r_0$  to be obtained by linear regression when the optimum value of  $n$  has been derived. The analytical solution

$$2\pi \int_0^\infty \sigma_0 r e^{-\left(\frac{r}{r_0}\right)^n} dr = \frac{2}{n} \pi \sigma_0 \Gamma\left(\frac{2}{n}\right) r_0^2, \quad (7)$$

then yields an estimate of the total luminous flux within the pass-band concerned.

Clearly, this generalisation incorporates not only the  $r^{\frac{1}{4}}$  law ( $n = \frac{1}{4}$ ) but also exponentials ( $n = 1$ ) and Gaussians ( $n = 2$ ) as well as both intermediate and more extreme cases. Although it is a one-component model, galaxies exhibiting two-component [or yet more complicated] structure can be comfortably accommodated by this scheme after their images have been smoothed sufficiently.

For the benefit of readers wishing to use this extrapolation system, a listing of the relevant FORTRAN code can be found in Appendix A. The subroutine EXTRAPOL.FOR: (1) increments the profile-curvature parameter  $n$ , and attempts (for each  $n$ ) to fit Sérsic's law to a surface-brightness profile defined by elliptical isophotes ( $r_i, \mu_i(r), \sigma_{\mu_i(r)}$ ); (2) quantifies the quality of the fit obtained for each value of  $n$ ; and (3) integrates the volume beneath the surface defined by the best-fitting profile form (after rotation through  $2\pi$  radians about  $r = 0$ ) to  $r = \infty$ , thereby yielding a total-magnitude estimate. It calls the subroutine FIT and the function GAMMLN, both from Press et al. (1986). Note that FIT actually fits a straight line of the form  $Y = A + BX$ , not one of the form  $Y = AX + B$ . Also, in order to reduce the dependence on other subroutines and functions, we removed the lines:

Q=1. and Q=GAMMQ(0.5\*(NDATA-2),0.5\*CHI2),

from this subroutine and removed the parameter Q from Line 1.

Although *t*-system total magnitudes cannot generally be derived directly from high resolution surface photometry of bright galaxies in the literature, they can be derived from surface photometry of virtually all galaxies fainter than  $B_{25} \sim 15$  mag. provided that the resolution of the photometry [after smoothing] is coarser than about  $4''.5$  (FWHM). In the compilation of their VPC, Young & Currie (in press) found that a reasonable amount of smoothing of their plate-scan data was necessary simply in order to prevent the fragmentation of images during the image segmentation process. They found that the minimum degree of smoothing required by the segmentation software was

actually sufficient for the derivation of *t*-system total magnitudes from the surface-brightness profiles of all unsaturated galaxies with enough isophotes above the limiting one for the fits to be performed.

#### 4. System stability

In this section, we test the stability of the *t* system with respect to morphological type, size of atmospheric seeing disc, degree of smoothing and limiting isophote. These tests are based on CCD surface photometry of four galaxies of different morphological types. Details of the original observations and of the early stages of the reduction procedures are listed and/or referenced below for each galaxy individually.

*Spiral (Sbc) at:  $(\alpha, \delta)_{1950.0} = 22^{\text{h}}01^{\text{m}}06^{\text{s}}, -20^{\circ}07'24''$ .* One 200-s *B*-band exposure of this galaxy was used; the frame having been taken in 1989 using the RCA CCD chip at the prime focus of the 2.5-m Isaac Newton Telescope. The FWHM of the seeing disc at the time of observation was  $1''.1$ . A  $300 \times 300$   $0''.741$ -pixel subsection of the field was used after being cleaned of stars and other galaxies. For details of the reduction and calibration procedures adopted, see Metcalfe et al. (1995).

*Lenticular: NGC 7180.* One 600-s *B*-band exposure of this galaxy was used; the frame having been taken in 1989 with the TI CCD chip on the 0.9-m telescope of the Cerro Tololo Inter-American Observatory. The FWHM of the seeing disc was about  $1''.5$ . The original  $396 \times 396$  array of  $0''.494$  pixels was binned up to a  $197 \times 197$  array of  $0''.988$  pixels [by omitting the peripheral pixels in the original array]. A  $120 \times 120$  subsection of the resulting frame was then used after it had been cleaned of stars and other galaxies. For details of the reduction and calibration procedures adopted, see Metcalfe et al. (1995).

*Classical elliptical: NGC 6411.* One 200-s *B*-band exposure of this galaxy was used; the frame having been taken using a Loral CCD at the prime focus of the 4.2-m William Herschel Telescope on La Palma. The observation was made at UT 22:08 on 1997 September 4, when the FWHM of the seeing disc was  $1''.1$ . Stellar images on the frame were removed using Starlink's GAIA package and the photometric zero point was based on observations of Landolt (1983) standard stars. The original  $2048 \times 2048$  array of  $0''.26$  pixels was binned up to a  $512 \times 512$  array of  $1''.02$  pixels. A  $360 \times 360$  pixel subsection of the binned-up array was then used.

*Dwarf elliptical: NGC 147.* This galaxy is a member of the Local Group and lies within the vicinity of M31. Nine 600-s and four 900-s exposures of this galaxy were made of it using the CCD camera on the 60/90-cm F/3 Schmidt Telescope of Beijing Astronomical Observatory's (hereunder BAO) Xing Long Station. The observations were made between UT 14:03 and 17:08 on 1996 October 18, when the FWHM of the seeing disc was  $2''.6$ . The CCD chip used was a Ford device which had an array size

of  $2048 \times 2048$  pixels, and a corresponding field of view of  $54'37'' \times 54'37''$ . In the absence of a broad-band filter, an *i*-band Beijing-Arizona-Taipei-Connecticut (hereunder BATC) survey filter was employed. The BATC filter system is described at length by Fan (1995) and briefly by Fan et al. (1996) who refer to the *i*-band filter as Filter No. 9. This filter's transmission curve peaks at a wavelength of  $6600\text{\AA}$  and has a FWHM of  $480\text{\AA}$ . After bias subtraction, flat fielding and the removal of spurious images caused by cosmic-ray events; all thirteen CCD frames were stacked, thereby yielding a single frame whose effective integration time was 9000 s. The procedure adopted for these reductions was the same as adopted by Fan et al. (1996). As Hodge (1976) found no evidence for any global colour gradient in NGC 147, we were able to transform the *i*-band images directly to the *B* system by calibration with the  $r_{\text{TG}}$ -band surface-brightness profile of Kent (1987) and the transformation,  $B = r_{\text{TG}} + 1.21$  from Young & Currie (1994). After the calibration process, the stacked frame was binned up to one with  $15''.03$  pixels.

Although NGC 6411 and NGC 147 were not observed by Metcalfe et al. (1995), the same software as used by those authors was applied to the reduced but unsmoothed frames of these galaxies in order to generate Kron-system total magnitudes for them. The values obtained were  $B_K = 12.88$  and  $10.36$  respectively.

For each galaxy, four synthetic low-resolution images were generated. This involved the convolution of each original or stacked image with Moffat (1969) functions of  $(\sqrt{16 - d^2})''$ ,  $8''$ ,  $16''$  and  $32''$  FWHM in the case of the classical galaxies or with the same functions of  $1'$ ,  $2'$ ,  $4'$  and  $8'$  FWHM, in the case of NGC 147; where  $d$  was the FWHM of seeing disc at the time of the original observation(s). In order to minimize edge effects, each digital image was embedded in a very much larger array of pixels (in which each pixel in the surrounding grid was set to zero) before any convolution was performed.

The Moffat function was chosen on this occasion in order to simulate both the effect of poor seeing on nearby objects and the effect of average seeing on distant objects. Note that in adopting a Moffat function here, we are actually applying a very much more stringent test on the stability of the *t* system than we would have had we adopted the Gaussian function that we recommend for the purpose of smoothing. This is because the Moffat function is a much more complicated function than the Gaussian one, being similar to the Gaussian at small radial distances but falling off much more slowly at larger radial distances.

Godwin's (1976) image-segmentation software, as outlined by Carter & Godwin (1979), was used in order to fit elliptical isophotes of  $0.25 \text{ mag. arcsec}^{-2}$  separation (each defined by a mean radius  $r$ , an ellipticity and a position angle) to all of the synthetic low-resolution images. The isophotes were weighted according to the simple algorithm:  $\sigma_\mu = 0.05$  for  $\mu \leq 20.0$  or  $\sigma_\mu = 0.02(\mu - 20.0)$  for  $\mu > 20.0$ . The resulting synthetic surface-brightness

profiles are plotted in Fig. 1 together with the best fitting Sérsic model profiles; whilst the corresponding model parameters are tabulated in Table 1, which also lists those model parameters obtained when different limiting isophotes were applied.

As can be seen from Fig. 1 and Table 1, Sérsic's model yields very consistent results for all of the synthetic images except for the two highest resolution images of the classical elliptical (which, at 12th magnitude is in fact a very bright object) and the highest resolution image of the dwarf elliptical. In these three cases one-component profile models appear not to be completely adequate. However, once the resolution of a galaxy image has been degraded sufficiently, even if purely by seeing effects, the *t*-system total magnitudes obtained do appear to be stable typically to a couple of percent or so, irrespective of morphological type, the size of the seeing disc, or the limiting isophote—provided that the limiting isophote is not so bright that there are too few isophotes to fit.

Note that under normal circumstances, when the seeing disc is *not* almost as large as the galaxy image itself and the resolution of the image can be deliberately degraded by convolution with a Gaussian function (or even a simple Hanning function), the level of stability with respect to image resolution must be even greater than this. This is because the synthetic surface-brightness profile obtained by convolving any galaxy image with a Gaussian function of large FWHM, must be more Gaussian than the original profile and therefore more likely to be well described by Sérsic's law (as the Gaussian function, unlike the Moffat function for example, can be perfectly described by Sérsic's law).

We also tested the system for stability with respect to different weighting schemes for the isophotes, and found that whilst altering the weightings had very significant effects on the  $\chi^2$  values obtained, and reasonably significant effects on which best-fitting parameters were adopted, the effects on the total magnitude values obtained were only at the one or two per cent level—for realistic weighting schemes at least.

## 5. Comparisons with other systems

### 5.1. High-resolution images

In Table 2, we have transformed those CCD-system total-magnitude estimates flagged with a superscript 'b' symbol in Table 1 into Johnson or Cousins system magnitudes based on the colour equations of Metcalfe et al. (1995). Note that we did *not* invoke Metcalfe et al.'s magnitude values for any of the relevant galaxies, *only* their colour values when necessary.

It is clear from Table 2 that the agreement between the different systems for the objects considered is excellent. Note that for the three classical galaxies, the zero points on which the Kron-system and *t*-system values were based

**Table 1.** Best-fitting Sérsic model parameters for the synthetic seeing-distorted surface-brightness profiles depicted in Fig. 1, and for the same profiles but with brighter limiting isophotes

type	seeing FWHM/arcsec	limiting isophote /mag.arcsec <sup>-2</sup>	model parameters			$m_t$ /mag.	quality of fit <sup>a</sup>	
			$n$	$\mu_0$	$r_0$		$\chi^2$	$\nu$
S	4	$\mu_B(\text{CCD})=25.50$	1.20	20.90	0.920E+01	14.40	3.5961	17
	8	"	1.35	21.43	0.125E+02	14.41	0.8579	15
	16	"	1.39	22.11	0.172E+02	14.42	1.0134	12
	32	"	1.41	22.97	0.256E+02	14.44	0.1360	8
S	4	26.50	1.18	20.89	0.905E+01	14.40	3.9638	21
	8	"	1.29	21.39	0.120E+02	14.40	2.1809	19
	16	"	1.30	22.06	0.164E+02	14.41	2.2567	16
	32	"	1.26	22.87	0.235E+02	14.40	0.5753	12
S	4	27.50	1.20	20.91	0.922E+01	14.40	4.6817	25
	8	"	1.29	21.40	0.120E+02	14.40	2.2766	23
	16	"	1.27	22.03	0.160E+02	14.40	2.6476	20
	32	"	1.18	22.80	0.219E+02	14.38 <sup>b</sup>	1.0317	16
S0	4	$\mu_B(\text{CCD})=24.50$	0.93	19.20	0.521E+01	13.46	0.6036	18
	8	"	1.16	19.99	0.907E+01	13.47	0.5109	16
	16	"	1.34	20.92	0.150E+02	13.49	1.5291	13
	32	"	1.45	21.82	0.240E+02	13.45	0.1496	9
S0	4	25.50	0.96	19.25	0.549E+01	13.47	1.7091	22
	8	"	1.19	20.02	0.934E+01	13.47	0.9366	20
	16	"	1.29	20.89	0.146E+02	13.48	2.3516	17
	32	"	1.48	21.83	0.243E+02	13.46	0.3424	13
S0	4	26.50	0.98	19.28	0.569E+01	13.47	2.2644	26
	8	"	1.21	20.04	0.952E+01	13.47	1.5676	24
	16	"	1.29	20.89	0.146E+02	13.48	2.5165	21
	32	"	1.60	21.90	0.257E+02	13.47 <sup>b</sup>	2.7139	17
E	4	$\mu_B=26.00$	0.39	17.72	0.443E+00	12.81	45.6758	25
	8	"	0.55	19.33	0.296E+01	12.86	44.8807	22
	16	"	0.64	20.15	0.613E+01	12.86	4.9034	18
	32	"	0.85	21.50	0.181E+02	12.84	0.7091	14
E	4	27.00	0.37	17.54	0.323E+00	12.78	48.0880	29
	8	"	0.51	19.17	0.228E+01	12.81	53.6671	26
	16	"	0.60	20.01	0.507E+01	12.82	7.3776	22
	32	"	0.84	21.48	0.176E+02	12.84	0.7639	18
E	4	28.00	0.38	17.63	0.380E+00	12.80	51.2237	33
	8	"	0.51	19.17	0.229E+01	12.81	54.7888	30
	16	"	0.60	20.01	0.507E+01	12.82	8.2497	26
	32	"	0.86	21.52	0.185E+02	12.84 <sup>b</sup>	1.7321	22
dE	60	$\mu_B = 27.16$	0.89	22.73	0.110E+03	10.27	1.1096	15
	120	"	1.07	23.27	0.166E+03	10.29	0.2913	13
	240	"	1.35	24.09	0.278E+03	10.33	0.1603	11
	480	"	1.47	24.94	0.415E+03	10.40	0.0156	7
dE	60	28.16	0.96	22.83	0.123E+03	10.30	3.0475	19
	120	"	1.17	23.37	0.185E+03	10.32	1.3257	17
	240	"	1.38	24.10	0.283E+03	10.33	0.2436	15
	480	"	1.37	24.89	0.397E+03	10.37	0.1210	11
dE	60	29.16	1.07	22.98	0.145E+03	10.31	9.2790	23
	120	"	1.29	23.50	0.207E+03	10.32	4.0134	21
	240	"	1.43	24.13	0.290E+03	10.34	0.8021	19
	480	"	1.22	24.77	0.357E+03	10.34 <sup>b</sup>	0.8673	15

<sup>a</sup>  $\nu$  represents degrees of freedom (number of isophotes minus two)<sup>b</sup> These values were (after system transformation when relevant) adopted in Table 2

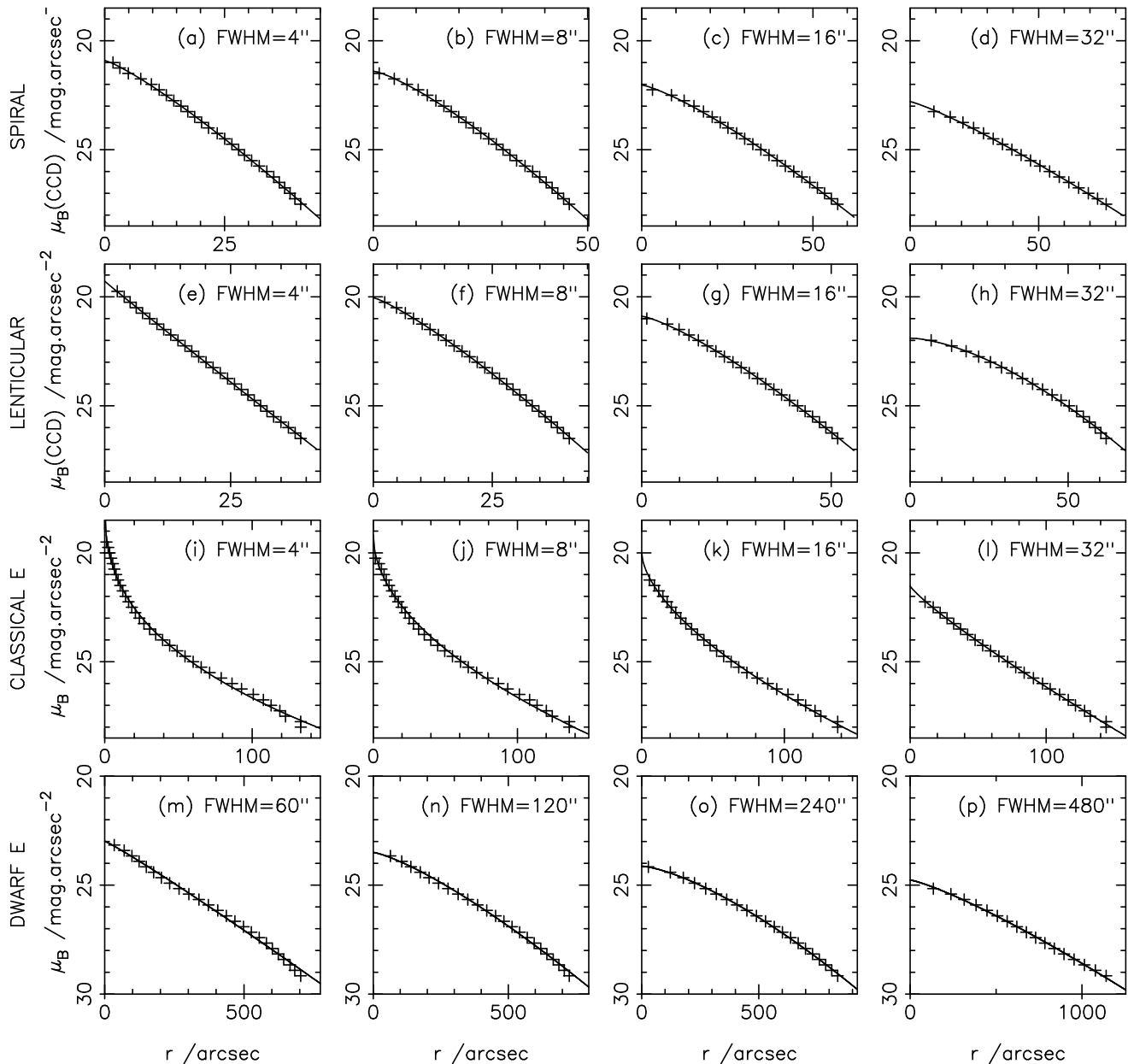


**Fig. 1.** The simulated effect of poor to very poor seeing conditions on the surface-brightness profiles of bright galaxy images: **(a, b, c and d)** a spiral, **(e, f, g and h)** a lenticular, **(i, j, k and l)** a classical elliptical and **(m, n, o and p)** a dwarf-elliptical galaxy. This effect is analogous to the effect of ordinary seeing conditions on more distant galaxies of the same type and physical size. The image resolution function adopted was that of Moffat (1969) and the FWHM of the synthetic seeing discs are shown in arcsec. The curves represent model Sérsic profiles fitted to all plotted isophotes.

were the same, whilst those on which the *T*-system values were based were independent. In the case of the dwarf elliptical though, the *T*-system and *t*-system values were both based on the zero point of Kent (1987).

For the sake of completeness, we would very much have liked to include a dwarf galaxy whose *n* value is much greater than 1.0 in the comparisons performed in this subsection. However, we have not yet been able to obtain

deep CCD images of a suitable galaxy. In any case, as mentioned in Section 2, there can be no doubt that such objects cannot be accommodated by the *T* system, which necessarily over-estimates their luminosities.

**Table 2.** A comparison between Johnson *B*-band total-magnitude values obtained from high-resolution galaxy images using different extrapolation systems

type	designation or $(\alpha, \delta)_{2000.0}$	$(B_T)^a$	$(m_B)^b$	$(B_K)^c$	$(B_t)^d$
Sbc	(22:03:51.2, −19:52:51)	N/A	14.41	14.49	14.47
S0	NGC 7180	13.56	13.61	13.67	13.65
E	NGC 6411	12.79	12.93	12.88	12.84
dE	NGC 147	10.47	10.43	10.36	10.34

<sup>a</sup> *T* system extrapolation of aperture and/or surface photometry, RC3

<sup>b</sup> Zwicky magnitude transformed to *T* system, RC3

<sup>c</sup> Kron system extrapolation, Metcalfe et al. (1995) or this work

<sup>d</sup> *t* system extrapolation, this work

### 5.2. Low-resolution images

Whilst the agreement between the three systems is very good for the four resolved galaxy images already investigated, let us now consider what would happen if we attempted to estimate the total magnitudes of these same galaxies if they were, hypothetically, re-located at much greater distances from our galaxy. Clearly, seeing effects would become more significant than they were during the original observations. In fact, the effects can be understood from Fig 1, if one interprets greater FWHM values as the same degree of seeing due to a particular galaxy being re-located to greater distances from us, and one re-scales the absolute radial-distance scales accordingly. For example, in the case of NGC 147, which is about 0.67 Mpc distant (Lee et al. 1993), Fig. 1(i-l inclusive) represents profiles under purely hypothetical atmospheric conditions in which the FWHM of the seeing discs are 60-480", but also represents the same galaxy if re-located at a distance of 13.6 Mpc and observed under conditions with seeing discs of 0"3-2"4 FWHM. As one would expect, the profiles of more distant and/or physically smaller galaxies are more susceptible to distortion by seeing effects than those of nearby and/or physically larger systems.

In the case of the *t* system, distortion of image profiles due to seeing effects can be accounted for, as was demonstrated in Section 4. However, because the *T* system assumes that a galaxy's surface-brightness profile [or the integrated luminosity equivalent] is only a function of morphological type and not of image resolution, it is therefore only applicable to highly-resolved galaxy images. As is evident from Table 3, if seeing effects are significant but not taken into account, this will generally result in an *over*-estimate of luminosity for a particular galaxy.

The Kron system, by contrast, does not make any prior assumption as to the profile shape of a target galaxy,

**Table 3.** *T*-system total magnitude estimates based on the synthetic classical elliptical galaxy profiles<sup>a</sup> plotted in Fig. 1 as a function of the FWHM of the seeing disc

limiting isophote $\mu_B/\text{mag.arcsec}^{-2}$	FWHM of seeing disc /arcsec			
	4	8	16	32
26.0	12.57	12.39	12.45	12.27
27.0	12.63	12.52	12.57	12.45
28.0	12.71	12.65	12.65	12.55

<sup>a</sup> For the sake of consistency, we used the same isophotal weighting scheme as for the *t*-system profile fitting procedure

though it does make a smaller assumption as to the shape of the curve representing the logarithmic derivative of the light-growth at large radial distances. We would therefore expect Kron-system total-magnitude scales to be very stable with respect to the size of the seeing disc, but there may of course still be room for small second order effects due to the assumption mentioned.

### 5.3. Images due to point sources

**Table 4.** Estimates of the total light contained under two typical [two-dimensional radially symmetric] Moffat surfaces, obtained by fitting different profile laws to different numbers of isophotal levels; the resulting values being quoted as linear fractions of the actual total-light values (which have both been set to unity)

law adopted	no. isophotal levels <sup>a</sup>	Hamburg Schmidt	Lick 120-inch
de Vaucouleurs $r^{\frac{1}{4}}$	8	6.391	6.315
"	16	1.823	1.808
"	24	1.443	1.363
"	32	1.552	1.349
Sérsic $r^n$	8	0.933	0.881
"	16	0.978	0.955
"	24	0.995	0.988
"	32	1.001	1.003
Gauss $r^2$	8	0.885	0.812
"	16	0.963	0.938
"	24	1.002	1.033
"	32	1.015	1.120

<sup>a</sup> The depth of the simulated surface-photometry in terms of the number of isophotal levels (of 0.25 mag.arcsec<sup>−2</sup> separation) fitted

In order to test the applicability of the *t* system to images due to point sources, we simulated the surface photometry one might expect to obtain for two model point spread functions. The two model profiles adopted were based on Moffat functions using the original parameter values quoted by Moffat (1969) for traced stellar images on Hamburg Schmidt and the Lick 120-inch reflector photographic plates. The adopted parameter values were  $\beta = 4$  and  $R = 5 \times 10^{-5}$ m for the Hamburg plates and  $\beta = 2.72$ , and  $R = 1.12 \times 10^{-4}$ m for the Lick plates. The brightest isophote in each case was taken to correspond to that radial distance,  $r$ , this time in metres, at which the surface brightness was  $0.125 \text{ mag.m}^{-2}$  fainter than the peak value at  $r = 0$ . Radii were then computed for further [circular] isophotes that were multiples of  $0.25 \text{ mag.m}^{-2}$  fainter than the brightest isophote.

The results of attempts to fit not only Sérsic's law, but also the Gaussian and  $r^{\frac{1}{4}}$  laws, to the brighter isophotes of these model profiles are shown in Table 4. For these fits, the adopted weighting scheme was:  $\sigma_{\mu} = 0.05 + 0.02(\mu_0 - \mu)$ , where  $\mu_0$  is the peak central surface brightness at  $r = 0$  in units of  $\text{mag.m}^{-2}$ . Note that although Moffat did not quote plate-scale values, we were still able to investigate the *fractional* differences between the extrapolated total-luminosity estimates and the true luminosities represented by the two-dimensional radially-symmetric Moffat surfaces<sup>2</sup>.

From Table 4, it is clear that, as one would expect, the  $r^{\frac{1}{4}}$  law always severely over-estimates the light due to a point-spread function represented by a Moffat profile. It is also evident from the same table that an extrapolation of Sérsic's model generally yields a significantly better estimate of the total light due to a typical point-spread function than does an extrapolation of a strictly Gaussian model.

In the above comparisons, we have of course applied a very stringent test to *t*-system and Gaussian-law extrapolations, by invoking pure Moffat functions to describe the unresolved images. In practice, as in the compilation of the VPC for example, the structures of the unresolved images should really be described by the product of three functions, the sampling function a Moffat function and the smoothing function, all convolved with one another. Provided that the smoothing function is a single-component function that falls off steeply with increasing radial distance, such as a Gaussian function, better results should be obtainable using Sérsic's model (or even a strictly Gaussian model) than those tabulated in Table 4. This is because a pure Moffat function is less amenable to being described by a Sérsic function (or the Gaussian case thereof) than is a Moffat function that has been deliberately smoothed. The *t* system is therefore applicable

to point-source galaxy images as well as resolved-galaxy images. While it cannot offer a perfect fit to a typical unsmoothed point-spread function, it does generally offer significantly better results than those that can be obtained by invoking a purely Gaussian model.

## 6. Summary

We have presented a new procedure for obtaining total-magnitude estimates from unsaturated galaxy images. This method involves first smoothing two-dimensional digital images numerically (ideally convolving them with a two-dimensional radially symmetric Gaussian function of sufficient FWHM), in order to produce lower-resolution images, which are then parameterised using elliptical isophotes. The rationale behind this is that even the faintest isophotes of the synthetic lower-resolution images (which cannot be measured accurately or at all in practice) become distorted in a predictable manner by the smoothing process. The second stage involves modeling the resulting surface-brightness profiles with Sérsic functions, and extrapolating the best-fitting functions to infinite radial distances. We have also demonstrated the system's high level of stability with respect to galaxy morphological type, limiting isophote and the size of the seeing disc (and thereby degree of smoothing too [provided one does not under-smooth], as typical smoothing functions cause distortions that are more easily accommodated by the fitting procedure than those distortions caused purely by seeing effects).

*Acknowledgements.* We would like to thank Jon Godwin for providing the photometry software and Steve Maddox for a useful discussion. This work made use of the computing facilities of the QSO & Observational Cosmology Group at BAO and those of Starlink. CKY gratefully acknowledges a PDRF from the National Postdoctoral Fellowship Office of China.

## References

- Carter D., Godwin J.G., 1979, MNRAS, 187, 711
- de Jong R.S., 1996, A&A, 313, 45
- de Vaucouleurs G., 1948, Ann. d'Astrophys., 11, 247
- de Vaucouleurs G., 1958, Handbuch der Physik, 53, 311, Springer-Verlag, Berlin
- de Vaucouleurs G., de Vaucouleurs A., Corwin H.G., 1976, Second Reference Catalog of Bright Galaxies, University of Texas, Austin
- de Vaucouleurs G., de Vaucouleurs A., Corwin H.G., Buta R.J., Paturel G., Fouque P., 1991, Third Reference Catalog of Bright Galaxies, Springer-Verlag, New York (RC3)
- Drinkwater M.J., Currie M.J., Young C.K., Hardy E., Yearsley J.M., 1996, MNRAS, 279, 595
- Fan X., 1995, MSc. Thesis, Chinese Academy of Sciences, BAO
- Fan X., Burstein D., Chen J. et al., 1996, AJ, 112, 628
- Godwin J.G., 1976, D.Phil. Thesis, University of Oxford
- Hodge P.W., 1976, AJ, 81, 25
- Hubble E., 1930, ApJ, 71, 131
- King I.R., 1966, AJ, 71, 64

<sup>2</sup> The latter surfaces having been integrated to very large radial distances using Simpson's rule with very small radial distance intervals.

- Kent S.M., 1987, AJ, 94 306  
 Kron R.G., 1980, Physica Scripta, 21, 652  
 Landolt A.U., 1983, AJ, 88, 439  
 Lee M.G., Freedman W.L., Madore B.F., 1993, ApJ, 417, 553  
 Maddox S.J. et al., 1990, MNRAS, 246, 433  
 Metcalfe N., Fong R., Shanks T., 1995, MNRAS, 274, 769  
 Metcalfe N., Shanks T., Fong R., Jones L.R., 1991, MNRAS, 249, 498  
 Moffat A.F.J., 1969, A&A, 3, 455  
 Press W.H., Flannery B.P., Teukolsky S.A., Vetterling W.T., 1986, Numerical Recipes, Cambridge University Press  
 Sersic J.L., 1968, Atlas de galaxias australes, Observatorio Astronomica, Cordoba  
 Vigroux L., Thuan T.X., Vader J.P., Lachieze-Rey M., 1986, AJ, 91, 70  
 Young C.K., 1994, D.Phil. Thesis, University of Oxford  
 Young C.K., 1997, In Galaxies: K.S. Cheng & K.L. Chan (eds.), Proceedings of the 21st Century Chinese Astronomy Conference, World Scientific, Singapore  
 Young C.K., Currie M.J., 1994, MNRAS, 268, L11  
 Young C.K., Currie M.J., 1995, MNRAS, 273, 1141  
 Young C.K., Currie M.J., A&AS, in press  
 Zwicky F., Herzog E., Wild P., 1961, Catalog of Galaxies and Clusters of Galaxies, 1, California Institute of Technology, Pasadena  
 Zwicky F., Herzog E., 1963, Catalog of Galaxies and Clusters of Galaxies, 2, California Institute of Technology, Pasadena  
 Zwicky F., Karpowicz M., Kowal C.T., 1965, Catalog of Galaxies and Clusters of Galaxies, 5, California Institute of Technology, Pasadena  
 Zwicky F., Herzog E., 1966, Catalog of Galaxies and Clusters of Galaxies, 3, California Institute of Technology, Pasadena  
 Zwicky F., Herzog E., 1968, Catalog of Galaxies and Clusters of Galaxies, 4, California Institute of Technology, Pasadena  
 Zwicky F., Kowal C.T., 1968, Catalog of Galaxies and Clusters of Galaxies, 6, California Institute of Technology, Pasadena

## Appendix A: FORTRAN code

```

SUBROUTINE EXTRAPOL
: (RMEANR,YMU,SIG,NDATA,
: SN,SMUO,SRO,TOTAL,SCHI2,NU)
* -----
* This subroutine fits Sersic profile parameters to a surface-brightness profile by chi squared minimisation. It then extrapolates the profile to obtain a t-system total magnitude estimate.
* -----
* INPUT PARAMETERS (all unchanged on output):
* RMEANR(100): mean radial distance of each isophote /arcsec;
* YMU(100): corresponding surface brightness of each isophote /mag.arcsec**(-2);
* SIG(100): corresponding 1 sigma uncertainty on each YMU;
* NDATA: number of isophotes (<101);
* -----

```

```

* OUTPUT PARAMETERS:
* SN, SMUO and SRO: best fitting Sersic parameters: n, mu_0 and r_0 respectively (see Equation 6);
* TOTAL: t-system total magnitude derived from the best fitting parameters;
* CHI2: chi squared value for adopted fit;
* NU: corresponding degrees of freedom.
* -----
* Two external routines called from Numerical Recipes, Press et al., Cambridge U.P. 1986:
* SUBROUTINE FIT (with the minor modifications described in Section 3) and
* FUNCTION GAMMLN (without modification).
* -----
REAL RMEANR(100), YMU(100), SIG(100),
: XMEANRN(100)
INTEGER NDATA(100)
DOUBLE PRECISION DRO, DNP1, GAMMLN
PI= 3.141592654
BCHI2= 100000.0
MWT= 1
* increment n from 0.2 to 3.0
DO I= 20,300
RN= 0.01*FLOAT(I)
DO J= 1,NDATA
XMEANRN(J)= (RMEANR(J))*RN
ENDDO
CALL FIT (XMEANRN,YMU,NDATA,SIG,MWT,
: FMUO,FSLOPE,SIGMUO,SIGS,CHI2)
* retain parameters of best fit so far
IF (CHI2.LE.BCHI2) THEN
BESTN= RN
BMUO= FMUO
BSLOPE= FSLOPE
BCHI2= CHI2
ENDIF
ENDDO
SCHI2= BCHI2
NU= NDATA-2
SN= BESTN
SMUO= BMUO
SRO= (1.086/BSLOPE)**(1.0/SN)
* evaluate total magnitude
DRO= DBLE(SRO)
DNP1= (2.0D0/DBLE(SN))
GAMP1= EXP(SNGL(GAMMLN(DNP1)))
TOTAL= -2.5*LOG10(2.0*PI*GAMP1/SN)
: +SMUO-2.5*SNGL(DLOG10(DRO**2D0))
END
* -----

```